

# Studies of Silicon–Nitrogen Ring Formation from Tetrachlorodisilanes

John L. Shibley, Robert West,\* and Douglas R. Powell

Department of Chemistry, University of Wisconsin, Madison, WI 53706-1396

Claire A. Tessier

University of Akron, Akron, OH 44325

Received 27 January 1994; revised, 7 March 1994

## ABSTRACT

The addition of  $n$  equiv of  $\text{MesNHLi}$  ( $n = 1, 2, 3, 4$ ) and  $m$  equiv of 12-crown-4 ( $m = 0.1, 1, 2, 3, 4$ ) to  $(\text{RSiCl}_2)_2$  ( $R = \text{Mesityl}; t\text{-Butyl}$ ) in THF at  $-78^\circ\text{C}$  resulted in higher yields and improved selectivities of cyclodisilazanes and azadisilacyclopropanes. The reaction of 2 equiv of  $\text{MesNDLi}$  with  $(\text{MesSiCl}_2)_2$  (**1**) yielded *cis*-2-chloro-1,2,3,4-tetramesitylcyclodisilazane (**2a**) with 95% Si–H deuteration. **2a** was quantitatively chlorinated with retention of stereochemistry by *N*-chlorosuccinimide to give the *cis* dichlorocyclodisilazane (**3**). Variable-temperature  $^1\text{H}$  NMR studies from  $-70^\circ\text{C}$  to  $25^\circ\text{C}$  in  $d_8\text{-THF}$  were performed on **1**, **2a**, **2b**, and **3**. **1** exhibited little variation throughout the temperature range, whereas **2a**, **2b**, and **3** showed several rotational isomers. *trans*-2,3-Bis(mesitylamino)-1,2,3-trimesitylazadisilacyclopropane was shown to isomerize to the *cis* isomer in the presence of *n*-BuLi or  $\text{MesNHLi}$ . The molecular structures of **1** and **3** were determined by X-ray crystallography. Compound **1** crystallized in the monoclinic space group  $P2_1/c$ , with cell parameters  $a = 16.599(2) \text{ \AA}$ ,  $b = 14.633(2) \text{ \AA}$ ,  $c = 16.945(2) \text{ \AA}$ ,  $\beta = 92.044(13)^\circ$ ,  $V = 4113.1(8) \text{ \AA}^3$ ,  $Z = 8$ ,  $d(\text{calcd}) = 1.409 \text{ g/cm}^3$ , and  $R = 6.88\%$ . Compound  $3 \cdot \text{C}_6\text{H}_6$  crystallized in the orthorhombic space group  $Pbca$ , with cell parameters  $a = 17.906(4) \text{ \AA}$ ,  $b = 13.918(3) \text{ \AA}$ ,  $c = 31.700(6) \text{ \AA}$ ,  $V = 7900(3) \text{ \AA}^3$ ,  $Z = 8$ ,  $d(\text{calcd}) = 1.194 \text{ g/cm}^3$ , and  $R = 7.52\%$ .

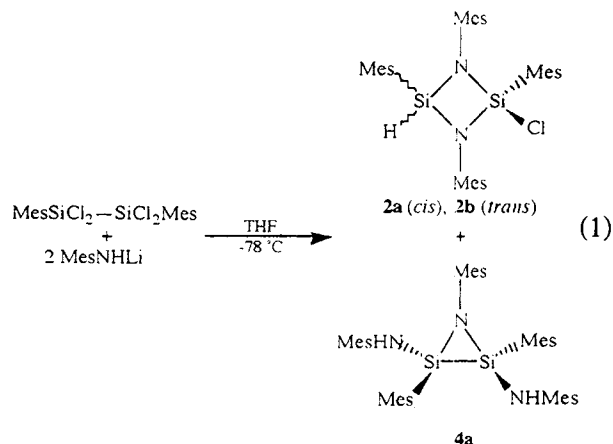
Dedicated to Prof. Adrian Gibbs Brook, father of the silicon-carbon double bond.

\*To whom correspondence should be addressed.

## INTRODUCTION

Tetrahalodisilanes have found only limited application as precursors to new organosilanes. Disilanes of the type  $(\text{RSiX}_2)_2$  ( $X = \text{halogen}$ ) are used in the synthesis of various polycyclic silanes [1]. Reactions of Grignard and lithium reagents with  $(\text{RSiCl}_2)_2$  have resulted in the exocyclic and endocyclic incorporation of the disilane fragment into C–Si ring systems [2]. Recently, a hexaaminodisilane was synthesized from a lithium amide and  $\text{Si}_2\text{Cl}_6$  without Si–Si bond cleavage [3], which is a common side reaction between amines and polychlorodisilanes [4].

Recently, we reported the surprising formation of two cyclodisilazanes (**2a**, **2b**) and an azadisilacyclopropane (**4a**) in the reaction of  $\text{MesNHLi}$  with  $(\text{MesSiCl}_2)_2$  (**1**)



(Equation 1) [5]. The formation and reactivity of cyclodisilanes [6] has been an intensely studied area,

whereas much less is known about azadisilacyclopropanes [7]. In order to investigate steric effects on the formation of these rings, we replaced  $(\text{MesSiCl}_2)_2$  with the bulkier disilane  $(t\text{-BuSiCl}_2)_2$  and found that both the rate of reaction and the product distribution are sensitive to this change [8]. In this article, we report results of further studies of the reaction of Equation 1, which bear on the pathway of this unusual ring formation process.

## EXPERIMENTAL SECTION

### General Considerations

All manipulations were performed using standard Schlenk techniques under an atmosphere of nitrogen or argon. All liquids were transferred using a syringe or cannula. Toluene, THF, diethyl ether, hexanes, and benzene were distilled from sodium benzophenone ketyl under nitrogen.  $\text{MesNH}_2$  was distilled under reduced pressure from NaOH prior to use. Infrared spectra were recorded on a Mattson Polaris FTIR spectrometer using NaCl plates.  $^{29}\text{Si}$  NMR spectra were obtained on a Bruker WP-270 spectrometer using INEPT pulse sequences and were referenced to external tetramethylsilane.  $^1\text{H}$  NMR spectra were recorded on a Bruker WP-200 spectrometer and were referenced to the residual solvent proton resonances that were calibrated against tetramethylsilane. Variable temperature  $^1\text{H}$  NMR experiments were performed on a Bruker WP-270 spectrometer. High resolution mass spectra were recorded on a Kratos MS-80 spectrometer. Reported melting points are uncorrected. *n*-BuLi in hexanes was titrated before use.  $(\text{MesSiCl}_2)_2$  [5] and  $(t\text{-BuSiCl}_2)_2$  [9] were prepared as described in the literature. *N*-chlorosuccinimide (NCS) was washed with ethyl alcohol and dried under vacuum prior to use. 12-crown-4 was dried over predried 4 Å molecular sieves. Lithium aluminum hydride (LAH) was purified from  $\text{Et}_2\text{O}$  prior to use.

### General Synthetic Procedure for Si–N Rings

$n$  MesNH<sub>2</sub> ( $n = 1\text{--}4$ ) was dissolved in THF (10 mL), and the solution was cooled to  $-78^\circ\text{C}$  in a dry ice/2-propanol bath.  $n$  *n*-BuLi ( $n = 1\text{--}4$ , 1.27 M) was added to the MesNH<sub>2</sub> solution and stirred for 45 minutes. The resulting MesNHLi solution was rapidly cannulated into a THF solution (10 mL) of  $(\text{RSiCl}_2)_2$  (0.4–0.6 mmol), also at  $-78^\circ\text{C}$ . The resulting reaction mixture was maintained at  $-78^\circ\text{C}$  for 30 minutes and slowly warmed to room temperature. The solvent was removed under reduced pressure, and the resulting colorless residue was redissolved in  $\text{Et}_2\text{O}$  or hexanes (10 mL). This solution was filtered under nitrogen and recrystallized from a minimum amount of hexanes. For  $\text{R} = \text{Mesityl}$ , the  $\text{Et}_2\text{O}$  insoluble portion was washed with benzene (15 mL) and then dried under vacuum.

### *cis*-2,4-Dichloro-1,2,3,4-tetramesitylcyclodisilazane (3)

*cis*-2-Chloro-1,2,3,4-tetramesitylcyclodisilazane (2a) [5] (0.40 g, 0.67 mmol) and NCS (0.13 g, 0.99 mmol) were dissolved in benzene (25 mL) and refluxed for 16 hours. The solution was orange after refluxing. The benzene was removed under vacuum, leaving an orange residue. Hexanes (20 mL) was added to the residue and the solution was gravity filtered. The yellow-orange solution was reduced in volume to ca. 5 mL and cooled to  $-20^\circ\text{C}$  to give 3 in an isolated yield of 0.18 g (43%, 0.28 mmol). Additional recrystallizations remove the remaining color but result in a lower yield. Analytical data for 3:  $^1\text{H}$  NMR ( $\delta$ , in  $\text{C}_6\text{D}_6$ ) 6.75 (s, 4 H), 6.47 (s, 2 H), 2.55 (s, 12 H), 2.13 (s, 6 H) 2.01 (s, 12 H), 1.88 (s, 6 H); INEPT  $^{29}\text{Si}$  NMR ( $\delta$ , in  $\text{C}_6\text{D}_6$ , 53.67 MHz vs. external TMS)  $-20.77$ ; exact mass for  $\text{C}_{36}\text{H}_{44}\text{N}_2\text{Si}_2\text{Cl}_2$ : calc  $m/e$  630.2420, found 630.2423; mp  $208\text{--}210^\circ\text{C}$ .

### 12-Crown-4 Studies

The general synthetic procedure was used. Ten mole percent and stoichiometric amounts of 12-crown-4 were used based on the amount of MesNH<sub>2</sub>. 12-Crown-4 was added via a syringe to the MesNH<sub>2</sub>/THF solution prior to cooling. *n*-BuLi was added after the solution was cooled to  $-78^\circ\text{C}$ . Crude product mixtures used in  $^1\text{H}$  and  $^{29}\text{Si}$  NMR studies were separated from LiCl. NMR spectra for the products were compared with those of pure compounds to establish their identities.

The presence of 12-crown-4 in the syntheses of the various Si–N rings resulted in some differences as compared to the syntheses without crown. In both cases, the addition of *n*-BuLi caused the MesNH<sub>2</sub>/12-crown-4/THF solution to become yellow, but the color disappeared eventually after addition to the disilane. LiCl precipitation occurred immediately when a stoichiometric amount of 12-crown-4 was added. Ten mole percent of crown resulted in delayed precipitation of much less LiCl than in the previous case but more than in the reactions without 12-crown-4.

### Reaction of *n*-BuLi and *trans*-2,3-Bis(mesitylamino)-1,2,3-trimesitylazadisilacyclopropane (4a)

4a (0.10 g, 0.15 mmol) was dissolved in THF (10 mL) and cooled to  $0^\circ\text{C}$ . *n*-BuLi (0.10 mL, 1.40 M) was added to the solution, which immediately became light yellow. The reaction mixture was stirred overnight and warmed to room temperature without any visible changes. The THF was removed under vacuum, leaving a pale yellow foam.  $^1\text{H}$  and  $^{29}\text{Si}$  NMR spectra showed a 1:1 ratio of 4a and *cis*-2,3-bis(mesitylamino)-1,2,3-trimesitylazadisilacyclopropane (4b). It was not possible to separate the

two isomers. Analytical data for **4b**:  $^1\text{H}$  NMR ( $\delta$ , in  $\text{C}_6\text{D}_6$ ) 6.71 (s, 4 H), 6.68 (s, 4 H), 6.46 (s, 2 H), 2.89 (s, 2 H), 2.86 (s, 6 H), 2.34 (s, 18 H). Because of the presence of **4a**, the remaining  $^1\text{H}$  NMR signals for **4b** could not be assigned; INEPT  $^{29}\text{Si}$  NMR ( $\delta$ , in  $\text{C}_6\text{D}_6$ , 53.67 MHz vs. external TMS)  $-42.92$ .

### Reaction of MesNDLi and **1**

MesND<sub>2</sub> was prepared by a modified literature procedure using +99.8% purity D<sub>2</sub> and +99.5 d<sub>1</sub>-ethyl alcohol [10]. Deuterium content was determined to be 95% based on the integration of the residual amine protons vs. the mesityl protons. The general procedure was used with 2 equiv of MesND<sub>2</sub>; the product (**2a**) was isolated and recrystallized twice from hot hexanes. The deuterium content at the Si–H position was determined by the integration of the residual Si–H vs. the aromatic protons and found to be 95%. The  $^1\text{H}$  NMR and mp of the product matched that of **2a**. The exact mass for  $\text{C}_{36}\text{H}_{44}^{29}\text{HN}_2\text{Si}_2\text{Cl}$ : calc  $m/e$  597.2872, found 597.2883.

### Variable-Temperature $^1\text{H}$ NMR Experiments

The solutions of **1**, **2a**, **2b**, and **3** were prepared using d<sub>8</sub>-THF predried over 4 Å molecular sieves and then sealed under vacuum. Each sample was cooled to  $-70^\circ\text{C}$  in the probe and allowed to reach thermal equilibrium before data acquisition. The sample was then warmed to the next temperature and allowed to reach thermal equilibrium. Data was collected for  $T = -70, -56, -44, -28, -17, -5$ , and  $25^\circ\text{C}$ . The samples were referenced to the residual methylene protons of THF at 3.58 ppm.

### X-ray Structure Determinations for **1** and **3**

X-ray crystallographic analyses were performed on a Siemens P4 diffractometer for **1** and a Siemens Pf3 diffractometer for **3** equipped with a graphite crystal monochromator and a Cu X-ray tube. Orientation matrices and unit cell parameters were determined by the least-squares fitting of 55 centered reflections ( $19^\circ < 2\theta < 55^\circ$ ) for **1** and 25 centered reflections ( $45^\circ < 2\theta < 50^\circ$ ) for **3**. Intensities of three check reflections were monitored every 50 reflections for **1** and every 100 reflections for **3** throughout the data collection. Structure solutions and refinements were performed using Siemens SHELXTL PLUS (SGI) for **1** and Siemens SHELXTL PLUS (VMS) for **3**. Details on crystal and intensity data collection are given in Table 1.

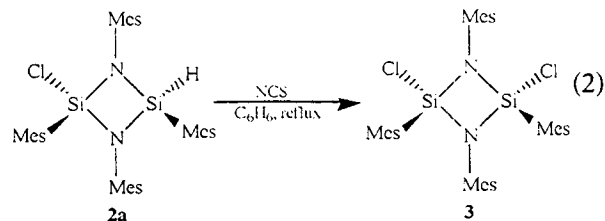
Suitable crystals of **1** were grown from a concentrated 10:1 hexanes/ether solution, whereas crystals of **3** were grown from concentrated hexanes at  $-20^\circ\text{C}$ . A colorless block-shaped crystal of **1** and a pale yellow block shaped crystal of **3** cut to the approximate dimensions of  $0.5 \times 0.5 \times 0.4$  mm and  $0.3 \times 0.3 \times 0.4$  mm, respectively, under

an argon blanket, were mounted on a thin glass thread with Paratone-N. The structures were solved by direct methods. In the final cycles of refinement, all nonhydrogens were assumed to vibrate anisotropically, and the hydrogen atoms were assumed to vibrate isotropically. Atomic coordinates and equivalent isotropic displacement coefficients for **1** are given in Table 4 and those for **3**, in Table 5.

## RESULTS AND DISCUSSION

### Synthesis of **3**

The chlorination of **2a** with NCS proceeded quantitatively to give the *cis* isomer, **3** (Equation 2). The structure of **3** was confirmed by X-ray crystallography. The Proton NMR spectrum of the crude reaction mixture showed only peaks that could be assigned to **3**, with no indication of the *trans* isomer, showing that the chlorination takes place stereospecifically. Introduction of the second chlorine atom resulted in a downfield shift of the  $^{29}\text{Si}$  NMR to  $-20.8$  ppm in **3**, relative to  $-25.2$  and  $-26.5$  ppm in **2a**. Attempts to chlorinate the *trans* isomer **2b** with NCS were unsuccessful, probably because the Si–H bond in this isomer is more hindered.



### Crystal Structure Determinations for **1** and **3**

In the crystal of **1**, two different forms were found to be present. Figures 1 (form A) and 2 (form B) use the same numbering scheme for clarity. Since A and B have very similar structures, the different views in Figures 1 and 2 accurately represent both forms. In both forms, the Si–Si bond distance was found to be 234.9 pm, which is nearly the same distance found in  $\text{Si}_2\text{Cl}_6$  [11]. Both forms have partially eclipsed mesityl rings with the C(1)–Si(1)–Si(2)–C(10) dihedral angles found to be  $49.1^\circ$  for A and  $51.3^\circ$  for B. In A, the C(9)–C(10) and C(9)–C(15) distances were 353.2 and 357.6 pm, respectively. For the other mesityl ring on A, the C(18)–C(1) and C(18)–C(6) distances were 363.5 and 357.4 pm, respectively. In B, the distances in pm for the equivalent carbon pairs were 386.9, 370.8, 348.8, and 362.9. In both cases, the shortest distances are less than the calculated van der Waals distance between a methyl group and a phenyl carbon of 370 pm [12].

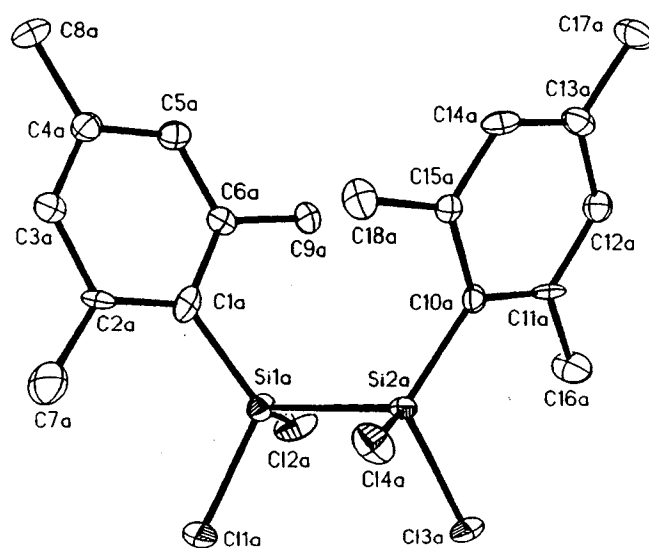
The crystal of **3** was found to contain eight disordered benzene molecules in the unit cell (Figure

**TABLE 1** Summary of Crystal Data Collection for **1** and **3**

	1	3
Empirical formula	$C_{18}H_{22}Cl_4Si_2$	$C_{36}H_{44}Cl_2N_2 \cdot C_6H_6$
Fw	436.3	709.9
Cryst syst	monoclinic	orthorhombic
Space group	$P2_1/c$	$Pbca$
<i>a</i> , Å	16.599(2)	17.906(4)
<i>b</i> , Å	14.633(2)	13.918(3)
<i>c</i> , Å	16.945(2)	31.700(6)
$\beta$ , deg	92.044(13)	
<i>V</i> , Å <sup>3</sup>	4113.1(8)	7900(3)
<i>Z</i>	8	8
<i>d</i> (calcd), g/cm <sup>3</sup>	1.409	1.194
Cryst size, mm	0.5, 0.5, 0.4	0.3, 0.3, 0.4
Color; habit	colorless block	light yellow block
Abs coeff, mm <sup>-1</sup>	6.484	2.314
F(000)	1808	3024
<i>T</i> , °C	−160(2)	−100(2)
2 $\theta$ range, deg	4.0 to 114.0	4 to 114
Scan type	2 $\theta$ – $\theta$	Wyckoff
Scan speed, deg/min	variable, 3 to 40	variable, 2 to 20
Scan range ( $\omega$ ), deg	1.60 plus $K_{\alpha}$ separation	0.70
Index ranges	$-18 \leq h \leq 18, 0 \leq k \leq 15, 0 \leq l \leq 18$	$0 \leq h \leq 19, 0 \leq k \leq 15, -34 \leq l \leq 0$
No. of reflns collected	4917	5930
No. of indep reflns	4917	5328
<i>R</i> , <i>R</i> <sub>w</sub> , %	6.88, 8.79	7.52, 8.89
Goodness of fit	1.86	1.88
Largest and mean $\Delta/\sigma$	0.001, 0	0.065, 0.015
Data-to-param ratio	8.4:1	8.7:1
Largest diff peak/hole, e Å <sup>-3</sup>	0.93/−0.90	0.41/−0.33

**TABLE 2** Selected Bond Distances (pm) for Compounds **1** and **3**

1		3	
Si(1A)–Si(2A)	234.9(3)	Si(1)–Cl(1)	208.6(2)
Si(1A)–Cl(1A)	205.8(3)	Si(1)–N(1)	173.9(5)
Si(1A)–Cl(2A)	205.9(3)	Si(1)–N(2)	174.3(5)
Si(1A)–Cl(3A)	206.3(3)	N(1)–C(10)	144.4(7)
Si(2A)–Cl(4A)	207.1(3)	Si(2)–C(19)	187.0(6)
Si(2A)–C(1A)	186.4(8)	Si(1)–C(1)	187.1(6)
Si(2A)–C(10A)	186.2(8)	N(1)–Si(2)	173.1(5)
Si(1B)–Si(2B)	234.9(3)	Si(2)–Cl(2)	208.1(2)
Si(1B)–Cl(1B)	206.8(3)	Si(2)–N(2)	174.4(5)
Si(1B)–Cl(2B)	206.1(3)	N(2)–C(28)	142.6(8)
Si(1B)–Cl(3B)	205.3(3)		
Si(2B)–Cl(4B)	206.5(3)		
Si(2B)–C(1B)	185.5(8)		
Si(2B)–C(10B)	188.2(8)		

**FIGURE 1** Thermal ellipsoid diagram of **1** (form A) showing 50% probability thermal ellipsoids. Hydrogen atoms are omitted for clarity.

3). The Si–Si distance was 251.9(2) pm, only 17 pm longer than in **1**; both nitrogens were planar. A surprising feature of the structure is the 17.1° dihedral angle between the Si(1)–N(1)–Si(2) and Si(1)–N(2)–Si(2) planes (Figure 4), as cyclodisilazanes, with few exceptions, are planar [13]. This large distortion is believed to be caused by the in-

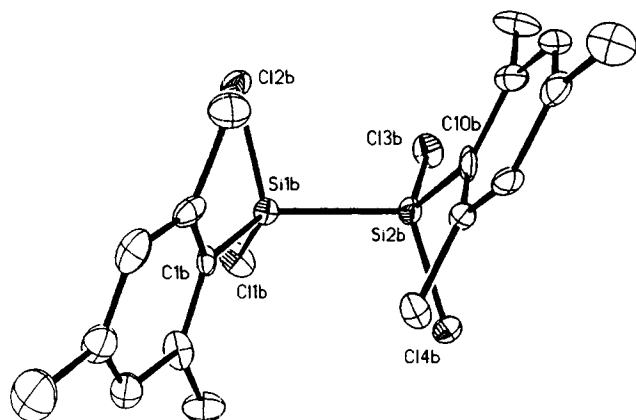


**FIGURE 2** Thermal ellipsoid diagram of **1** (form *B*) showing 50% probability thermal ellipsoids. Hydrogen atoms are omitted for clarity.

teractions between the *o*-methyl groups on the mesityl rings on silicon and the  $\pi$  system of both of the mesityl rings on nitrogen. The C(7)–C(28), C(9)–C(10), C(25)–C(10), and C(27)–C(28) distances were 316.4, 321.1, 315.8, and 316.9 pm, respectively; all the distances were shorter than the calculated van der Waals distance. Another indication of these interactions is that the mesityl ring on N(2) is bent toward the mesityl ring on Si(1) and likewise for the ring on N(1) toward the ring on Si(2), as evidenced by the bond angles (Table 3).

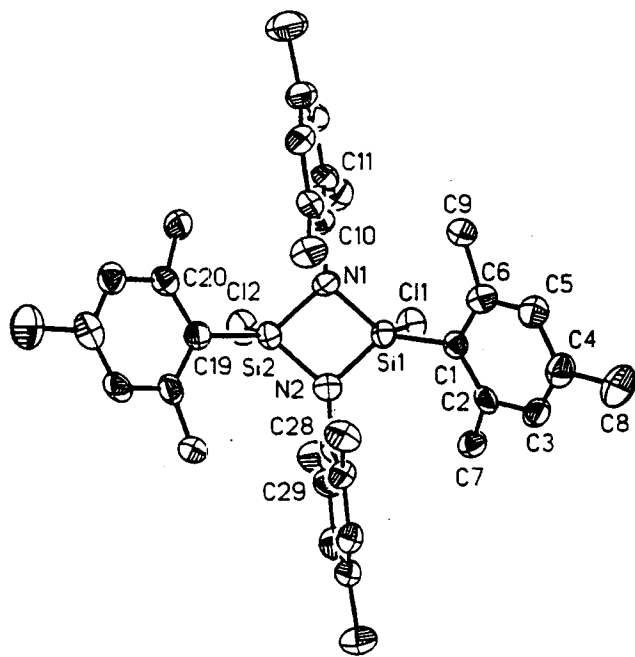


**FIGURE 3** Thermal ellipsoid diagram of **3** showing 50% probability thermal ellipsoids. Hydrogen atoms are omitted for clarity.

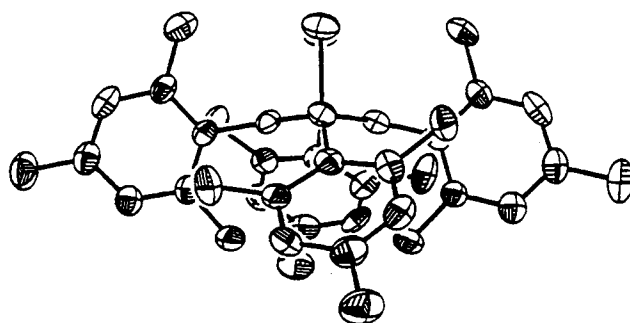


**FIGURE 4** Side view of **3** looking down the Si–Si axis. Hydrogen atoms have been omitted for clarity.

### Reaction of MesNHLi with **1**

The use of crown ethers to enhance reactivity of anions is well known [14], and this effect was also noticed in the reaction of MesNHLi with (RSiCl<sub>2</sub>)<sub>2</sub>. Two different ratios of 12-crown-4 were studied with varying amounts of MesNHLi in order to determine the effect of 12-crown-4 as well as the reactant ratio on product formation. These results are summarized in Table 6.

When **1** was treated with one equiv of MesNHLi in the absence of crown ether, **2a** and **2b** were formed in a 3:1 ratio (Equation 3).

**TABLE 3** Selected Bond Angles (deg) for Compounds **1** and **3**

	<b>1</b>	<b>3</b>
Si(2A)–Si(1A)–Cl(1A)	103.3(1)	Si(1)–N(2)–C(28) 130.3(4)
Cl(1A)–Si(1A)–Cl(2A)	102.1(1)	Si(1)–N(2)–Si(2) 92.5(2)
Cl(1A)–Si(1A)–Cl(1A)	116.3(3)	Si(2)–N(2)–C(28) 136.7(4)
Si(2A)–Si(1A)–Cl(2A)	107.0(1)	Si(1)–N(1)–C(10) 136.5(4)
Si(2A)–Si(1A)–Cl(1A)	114.9(2)	C(10)–N(1)–Si(2) 130.3(4)
Cl(2A)–Si(1A)–Cl(1A)	112.0(2)	Si(1)–N(1)–Si(2) 93.1(2)
Si(1A)–Si(2A)–Cl(3A)	104.2(1)	Cl(1)–Si(1)–C(1) 103.9(2)
Cl(3A)–Si(2A)–Cl(4A)	101.6(1)	Cl(1)–Si(1)–N(2) 110.5(2)
Cl(3A)–Si(2A)–C(10A)	115.3(2)	N(1)–Si(1)–N(2) 85.8(2)
Si(1A)–Si(2A)–Cl(4A)	106.5(1)	C(1)–Si(1)–N(2) 119.0(3)
Si(1A)–Si(2A)–C(10A)	115.5(2)	Cl(1)–Si(1)–N(1) 110.1(2)
Cl(4A)–Si(2A)–C(10A)	112.3(2)	Cl(2)–Si(2)–C(19) 103.8(2)
Si(2B)–Si(1B)–Cl(1B)	105.3(1)	N(1)–Si(2)–N(2) 86.0(2)
Cl(1B)–Si(1B)–Cl(2B)	102.0(1)	C(19)–Si(2)–N(2) 126.0(3)
Cl(1B)–Si(1B)–Cl(1B)	113.6(2)	N(1)–Si(2)–Cl(2) 110.5(2)
Si(2B)–Si(1B)–Cl(2B)	103.8(1)	N(1)–Si(2)–C(19) 119.5(3)
Si(2B)–Si(1B)–C(1B)	118.4(2)	Cl(2)–Si(2)–N(2) 110.2(2)
Cl(2B)–Si(1B)–C(1B)	112.1(2)	C(1)–Si(1)–N(1) 126.7(3)
Si(1B)–Si(2B)–Cl(3B)	101.6(1)	
Cl(3B)–Si(2B)–Cl(4B)	103.4(1)	
Cl(3B)–Si(2B)–C(10B)	116.3(3)	
Si(1B)–Si(2B)–Cl(4B)	108.4(1)	
Si(1B)–Si(2B)–C(10B)	114.3(3)	
Cl(4B)–Si(2B)–C(10B)	111.8(3)	

**TABLE 4** Atomic Coordinates ( $\times 10^5$ ) and Equivalent Isotropic Displacement Coefficients ( $\text{pm}^2$ ) for 1

Atom	x	y	z	$U(\text{eq})^a$
Si(1A)	19,434(12)	20,304(14)	18,723(12)	167(6)
Si(2A)	25,173(11)	34,913(14)	17,744(12)	147(6)
Cl(1A)	12,796(11)	21,202(15)	28,724(11)	283(7)
Cl(2A)	28,558(12)	11,524(14)	22,268(12)	308(7)
Cl(3A)	31,217(11)	36,805(15)	28,472(11)	298(7)
Cl(4A)	15,793(11)	44,168(13)	18,489(12)	258(6)
C(1A)	13,952(43)	16,223(48)	9,602(48)	192(25)
C(2A)	5,428(43)	15,927(52)	8,641(44)	168(24)
C(3A)	2,015(45)	13,245(55)	1,295(48)	236(26)
C(4A)	6,624(45)	10,882(54)	-5,032(49)	224(26)
C(5A)	14,972(44)	11,505(51)	-4,222(47)	201(26)
C(6A)	18,621(42)	13,929(47)	3,023(46)	151(23)
C(7A)	-276(45)	18,360(67)	14,956(53)	365(31)
C(8A)	2,657(48)	8,109(62)	-12,847(47)	307(28)
C(9A)	27,845(41)	13,950(53)	3,158(48)	221(26)
C(10A)	31,273(40)	36,871(49)	8,889(44)	142(23)
C(11A)	39,778(43)	36,502(52)	8,843(44)	171(24)
C(12A)	43,758(42)	38,280(53)	1,971(47)	200(25)
C(13A)	39,684(43)	40,139(55)	-5,171(47)	205(25)
C(14A)	31,383(42)	39,819(52)	-5,143(45)	176(24)
C(15A)	27,039(41)	38,300(47)	1,529(44)	132(23)
C(16A)	45,061(44)	34,084(64)	16,130(48)	309(29)
C(17A)	44,134(44)	42,350(61)	-12,465(47)	280(28)
C(18A)	17,953(41)	38,172(54)	494(48)	219(26)
Si(1B)	-29,396(11)	33,608(14)	38,020(12)	156(6)
Si(2B)	-24,142(12)	18,776(14)	36,913(13)	180(7)
Cl(1B)	-35,111(11)	36,275(15)	27,224(12)	310(7)
Cl(2B)	-19,373(11)	41,885(13)	37,661(12)	267(6)
Cl(3B)	-17,484(11)	19,927(14)	26,979(12)	269(6)
Cl(4B)	-33,417(11)	10,111(13)	33,409(12)	262(6)
C(1B)	-35,665(41)	36,255(49)	46,576(45)	156(23)
C(2B)	-44,169(46)	35,583(54)	46,288(43)	195(25)
C(3B)	-48,458(48)	37,804(53)	52,770(49)	252(28)
C(4B)	-44,822(49)	40,519(59)	59,899(55)	302(29)
C(5B)	-36,589(49)	40,605(57)	60,382(50)	281(29)
C(6B)	-31,915(46)	38,436(51)	54,043(50)	216(26)
C(7B)	-48,955(46)	31,975(62)	39,019(48)	316(29)
C(8B)	-49,759(58)	42,814(71)	66,934(61)	478(37)
C(9B)	-22,764(46)	38,016(61)	55,593(51)	314(30)
C(10B)	-18,615(46)	14,520(50)	46,081(50)	228(26)
C(11B)	-10,164(43)	13,490(56)	46,836(49)	227(27)
C(12B)	-6,856(44)	10,653(54)	54,197(50)	240(27)
C(13B)	-11,478(45)	8,962(53)	60,740(49)	233(26)
C(14B)	-19,748(42)	10,152(52)	59,872(49)	200(25)
C(15B)	-23,431(41)	12,901(50)	52,737(46)	162(24)
C(16B)	-4,339(44)	15,184(67)	40,441(52)	353(31)
C(17B)	-7,702(47)	5,961(61)	68,465(48)	307(29)
C(18B)	-32,492(43)	13,702(55)	52,585(49)	236(27)

<sup>a</sup>Equivalent isotropic  $U$  defined as one-third the trace of the orthogonalized  $U_{ij}$  tensor.

**TABLE 5** Atomic Coordinates ( $\times 10^5$ ) and Equivalent Isotropic Displacement Coefficients ( $\text{pm}^2$ ) for 3

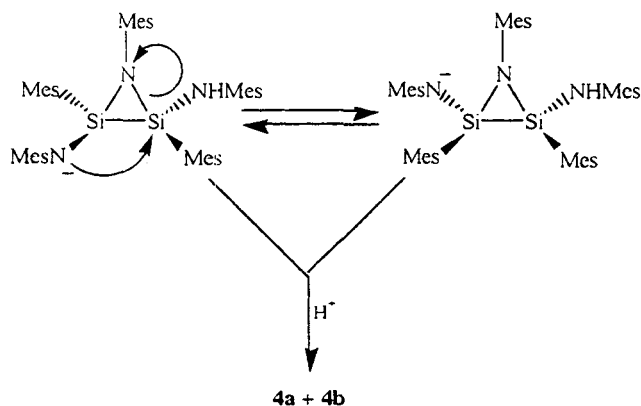
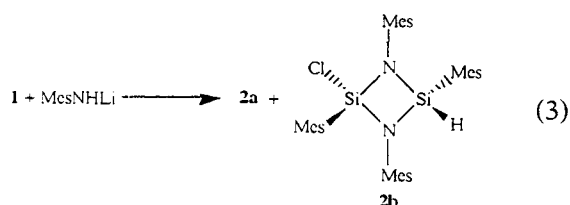
Atom	x	y	z	$U(\text{eq})^a$	occ
Si(1)	10,289(1)	2,014(1)	5,866(1)	34(1)	
Cl(1)	9,181(1)	1,913(1)	5,668(1)	49(1)	
C(1)	10,819(3)	1,322(4)	5,458(2)	33(2)	
C(2)	10,797(4)	314(5)	5,463(2)	37(2)	
C(3)	11,290(4)	-200(5)	5,204(2)	44(2)	
C(4)	11,775(4)	247(5)	4,930(2)	48(3)	
C(5)	11,743(3)	1,232(5)	4,899(2)	42(2)	
C(6)	11,267(3)	1,775(4)	5,150(2)	37(2)	
C(7)	10,227(4)	-272(4)	5,703(2)	48(3)	
C(8)	12,315(4)	-334(5)	4,666(3)	63(3)	
C(9)	11,211(4)	2,839(4)	5,050(2)	53(3)	
N(1)	10,477(3)	3,174(3)	6,040(2)	32(2)	
C(10)	10,680(3)	4,079(4)	5,849(2)	34(2)	
C(11)	10,148(4)	4,713(5)	5,687(2)	40(2)	
C(12)	10,375(4)	5,606(5)	5,547(2)	48(3)	
C(13)	11,123(4)	5,883(5)	5,538(2)	47(3)	
C(14)	11,642(4)	5,233(4)	5,684(2)	42(2)	
C(15)	11,441(3)	4,331(4)	5,843(2)	37(2)	
C(16)	9,333(4)	4,457(5)	5,683(2)	56(3)	
C(17)	11,347(5)	6,880(5)	5,396(3)	69(3)	
C(18)	12,039(3)	3,654(5)	5,996(2)	44(2)	
Si(2)	10,355(1)	2,872(1)	6,565(1)	35(1)	
Cl(2)	9,288(1)	3,246(1)	6,767(1)	55(1)	
C(19)	10,982(3)	3,410(4)	6,974(2)	36(2)	
C(20)	11,126(4)	4,398(5)	6,973(2)	40(2)	
C(21)	11,689(4)	4,781(5)	7,232(2)	43(2)	
C(22)	12,096(4)	4,208(5)	7,499(2)	50(3)	
C(23)	11,899(4)	3,251(5)	7,539(2)	43(2)	
C(24)	11,343(4)	2,846(5)	7,289(2)	43(2)	
C(25)	10,654(4)	5,128(5)	6,732(2)	56(3)	
C(26)	12,713(4)	4,646(6)	7,771(2)	63(3)	
C(27)	11,111(5)	1,832(5)	7,389(2)	61(3)	
N(2)	10,369(3)	1,681(4)	6,395(2)	35(2)	
C(28)	10,488(3)	760(5)	6,580(2)	35(2)	
C(29)	9,901(4)	252(5)	6,759(2)	42(2)	
C(30)	10,034(4)	-663(5)	6,925(2)	53(3)	
C(31)	10,748(4)	-1,087(5)	6,903(2)	46(3)	
C(32)	11,322(4)	-537(5)	6,739(2)	43(2)	
C(33)	11,210(3)	880(4)	6,577(2)	37(2)	
C(34)	9,113(4)	659(5)	6,771(2)	60(3)	
C(35)	10,880(5)	-2,099(5)	7,064(3)	72(3)	
C(36)	11,871(3)	951(5)	6,423(2)	46(2)	
C(1SA)	6,070(12)	3,302(14)	1,315(6)	70(1)	0.599(15)
C(2SA)	5,903(11)	2,399(16)	1,256(6)	70(1)	0.599(15)
C(3SA)	6,451(15)	1,706(14)	1,214(5)	70(1)	0.599(15)
C(4SA)	7,215(12)	1,965(18)	1,225(5)	70(1)	0.599(15)
C(5SA)	7,352(11)	2,913(18)	1,317(6)	70(1)	0.599(15)
C(6SA)	6,807(13)	3,544(14)	1,342(6)	70(1)	0.599(15)
C(1SB)	5,857(17)	3,011(23)	1,318(9)	70(1)	0.401(15)
C(2SB)	6,073(19)	2,073(23)	1,216(9)	70(1)	0.401(15)
C(3SB)	6,810(23)	1,735(21)	1,233(8)	70(1)	0.401(15)
C(4SB)	7,381(17)	2,414(27)	1,257(9)	70(1)	0.401(15)
C(5SB)	7,208(18)	3,370(25)	1,361(8)	70(1)	0.401(15)
C(6SB)	6,468(20)	3,727(20)	1,361(8)	70(1)	0.401(15)

<sup>a</sup>Equivalent isotropic  $U$  defined as one-third the trace of the orthogonalized  $U_{ij}$  tensor.

**TABLE 6** Effect of 12-Crown-4 on the Yields of Si–N Rings<sup>a</sup>

<i>n</i>	<i>m</i>	<i>(MesSiCl<sub>2</sub>)<sub>2</sub> + n MesNHLi + m 12-crown-4</i>			
		<b>2a</b>	<b>2b</b>	<b>4a</b>	<b>4b</b>
1	0	[27]	[9]	[0]	[0]
1	0.1	[33]	[11]	[0]	[0]
2	0	21	4	26	0
2	0.2	38			
		(57)	(19)	(5)	(0)
2	2	29			
		(45)	(15)	(10)	(0)
3	0			36	0
		[0]	[0]	[60]	[20]
3	0.3			44	0
		[0]	[0]	[65]	[20]
3	3			44	0
		[0]	[0]	[65]	[20]
4	0			43	0
		[0]	[0]	[80]	[10]
4	0.4			17	
4	4			0	
<i>n</i>	<i>m</i>	<i>(<i>t</i>-BuSiCl<sub>2</sub>)<sub>2</sub> + n MesNHLi + m 12-crown-4</i>			
		<b>6a + 6b</b>			
2	0	35			
		[45]			
2	0.2	30			
2	2	17			

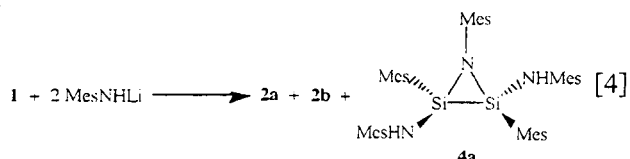
<sup>a</sup>The [ ] indicate conversions based on <sup>1</sup>H NMR. The ( ) indicate yield of crude compound.

**SCHEME 1**

Addition of 10 mol% 12-crown-4 improved the isolated yield of **2a** and **2b** without affecting the isomer ratio. In both reactions, about 0.5 equiv of **1**

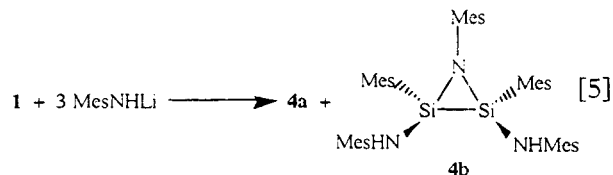
remained unreacted, and there was no evidence of Si<sub>2</sub>N ring formation by <sup>1</sup>H NMR.

The reaction of **1** and **2** equiv of MesNHLi without 12-crown-4 led to the formation of three major ring products, **2a**, **2b**, and **4a**, along with unreacted starting material. The use of 10 mol% 12-crown-4 resulted in a 75% yield of a mixture of **2a**, **2b**, and **4a** (~5%). Increasing the



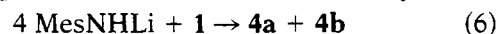
amount of crown ether lowered the isolated yield of **2a** while increasing the amount of **4a** (~10%). In both cases, **1** was completely consumed, as determined by <sup>1</sup>H and <sup>29</sup>Si NMR spectroscopy of the reaction mixtures.

The use of 3 equiv of MesNHLi without 12-crown-4 led to a quite different



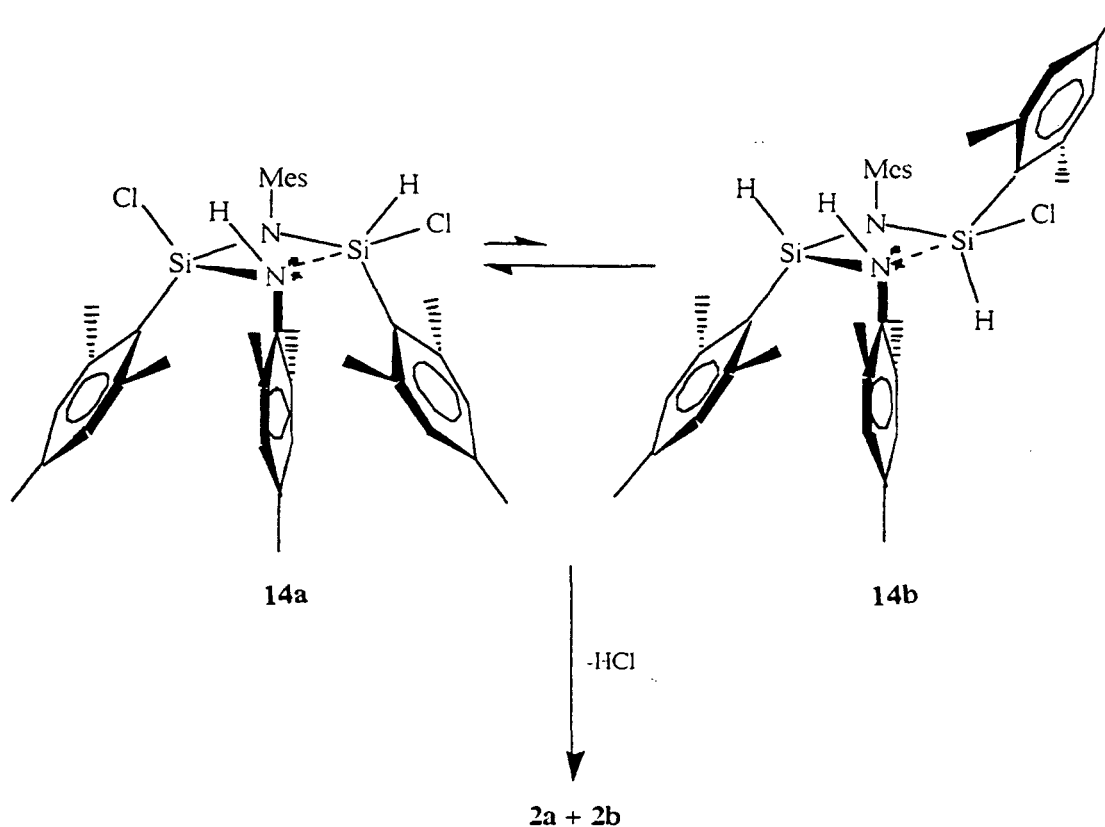
result (Equation 5). Isomers **4a** and **4b** were formed in an approximate 3:1 ratio; no **2a**, **2b**, or **1** were detected in the <sup>1</sup>H or <sup>29</sup>Si NMR spectra. Only one other silicon-containing product was found in the <sup>29</sup>Si NMR spectrum, whereas <sup>1</sup>H NMR showed several other compounds in small amounts. It was not possible to separate **4b** from **4a** by recrystallization. The addition of either 10 mol% or 3 equiv of 12-crown-4 ether slightly improved the yield of **4a**. The formation of **4b** appears to arise from the isomerization of **4a** in the presence of a base; this hypothesis was confirmed by treating **4a** with 1 or 2 equiv of *n*-BuLi. In both cases, 1:1 mixtures of **4a** and **4b** resulted. A possible mechanism for the isomerization, involving deprotonation, attack of the amide nitrogen on the remote silicon, and breaking of a Si–N ring bond, is illustrated in Scheme 1. Other pathways cannot be excluded.

Contrary to our previous report [5], the reaction of 4 equiv of MesNHLi with **1** actually



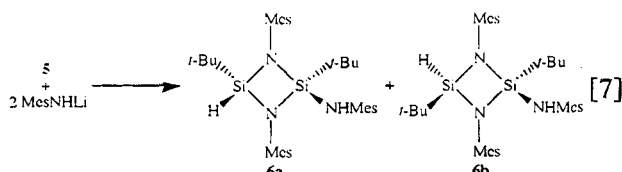
led to the formation of some **4b** as well as **4a**. Originally, **4b** was not detected by <sup>29</sup>Si NMR spectroscopy, but reexamination of the <sup>1</sup>H NMR spectrum of the reaction mixture showed that ~10% of **4b** was present. Use of 10 mol% 12-crown-4 resulted in a decrease in the yield of **4a** and an increase in the amounts of decomposition products, whereas 4 equiv of 12-crown-4 led only to the formation of various decomposition products.

The effect of steric hindrance on ring formation can clearly be seen when (*t*-BuSiCl<sub>2</sub>)<sub>2</sub> (**5**) is used



SCHEME 2

in place of **1**. In this case, the use of 12-crown-4 resulted in a lower



combined yield of **6a** and **6b**. These data indicate that the increased reactivity of crown-ether complexed MesNHLi does not completely overcome the steric hindrance at silicon.

### Reaction Pathway

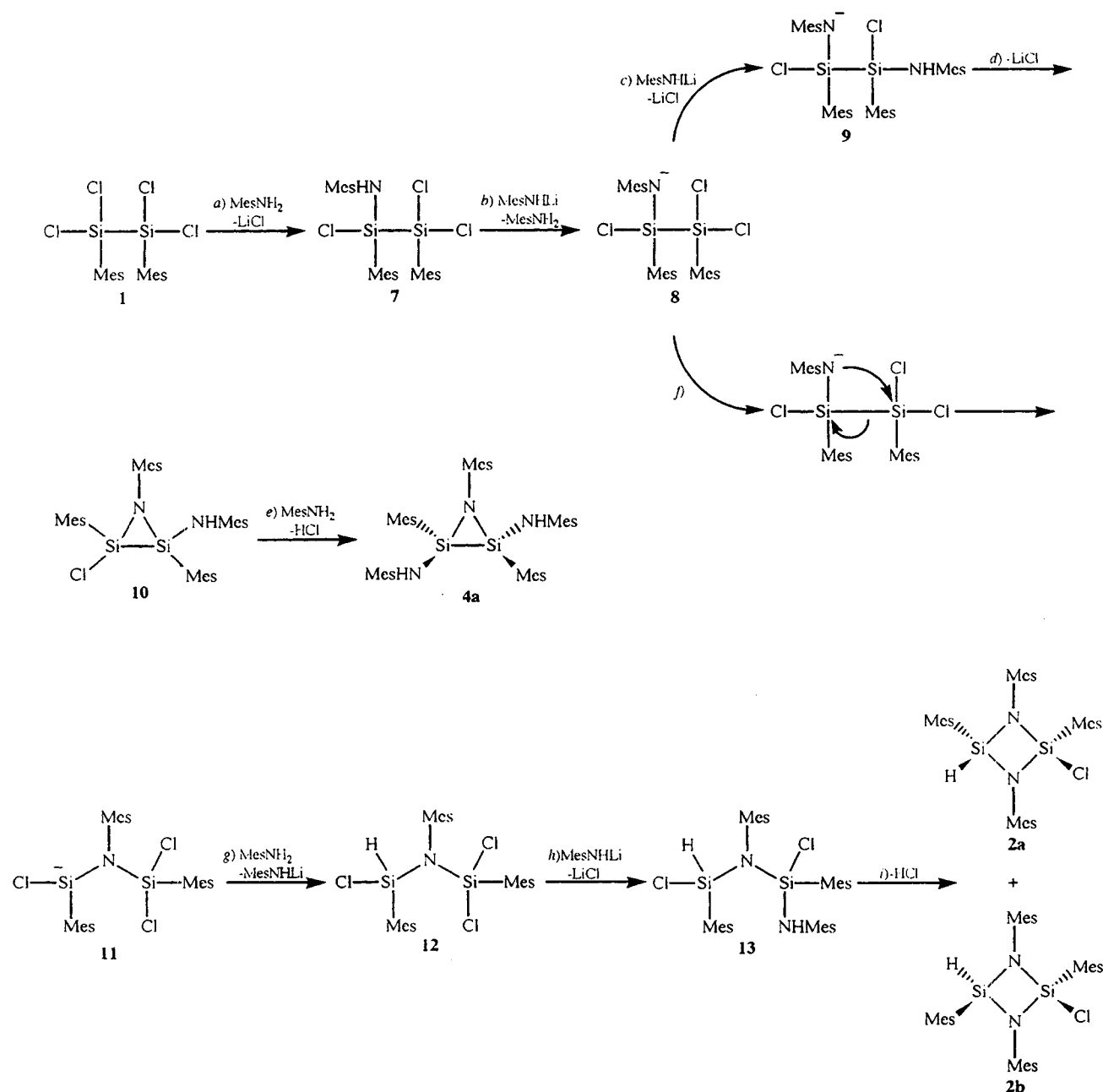
To put these new results and our previous results into perspective, a more complete reaction pathway is proposed, the first step being an addition of MesNHLi to **1** (Scheme 3). The second step is the deprotonation of the aminodisilane **7** (step *b*). It should be noted that, at this point, 2 equiv of MesNHLi have been consumed and 1 equiv of MesNH<sub>2</sub> has been generated. At **8**, the reaction pathway can branch. If sufficient MesNHLi is present, substitution occurs to yield a 1,2-diaminodisilane **9** (step *c*). Ring closure can then take place to form azadisilacyclopropane **11**. The MesNH<sub>2</sub> generated in step *b* can react with **10** to eliminate

HCl, giving **4a** [15]. The isomerization of **4a** by an anion can account for the observation of **4b** in the reaction mixtures (Scheme 1).

If the substitution reaction in step *c* cannot occur due to lack of lithium amide, the remaining lithium amidodisilane **8** can undergo an anionic rearrangement (step *f*). 12-Crown-4 most likely enhances the rate at which the formation of **8** occurs, but it has little effect on the anionic rearrangement in step *f*. After the formation of **11**, the silyl anion could deprotonate the MesNH<sub>2</sub> formed in step *b* (step *g*), regenerating an equivalent of MesNHLi. This step has been shown to be reasonable with the use of deuterium-labeled amine. When MesND<sub>2</sub> was used as the starting material, the Si-H bond in **2a** was found to be 95% deuterated. The regenerated MesNHLi can then react further to give the 1,3-disila-2,4-diazane **13** (step *h*). This compound can ring close via an HCl elimination to yield **2a** and **2b** (step *i*). This pathway is consistent with our results in Equation 7 [8].

Ring closure to **2a,b** could occur via two different pentacoordinate intermediates, **14a** and **14b** (Scheme 2). In **14a**, which leads to the *cis* isomer, **2a**, CH<sub>3</sub>/π interactions are maximized as is steric congestion. Both CH<sub>3</sub>/π interactions and steric hindrance are lower in **14b**. The 3:1 ratio may result from a competition between destabilizing steric congestion and stabilizing CH<sub>3</sub>/π interactions. **14a**





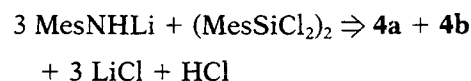
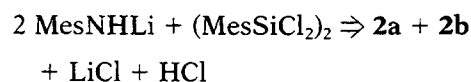
SCHEME 3

and **14b** are reasonable intermediates based on the known stereochemical behavior of silicon, although other possibilities cannot be ruled out [16]. This ring formation pathway is consistent with the isomer ratio being unaffected by 12-crown-4 and other reaction condition changes.

### SUMMARY

Our results show that the reaction of  $\text{MesNHLi}$  with  $(\text{MesSiCl})_2$  can be guided by controlling the ratio of reactants. With 2 equiv of  $\text{MesNHLi}$ , cyclodisi-

lazines are produced, whereas with 3 equiv of  $\text{MesNHLi}$ , the products are the 3-membered  $\text{Si}_2\text{N}$  rings. The net overall reactions can be summarized as follows:



Addition of small amounts (10 mol%) of 12-

crown-4 ether improves the yields in both reactions. The azadisilacyclopropanes **4a,b** are remarkably inert toward ring opening by lithium reagents.

## ACKNOWLEDGMENTS

This research was supported by a grant from the National Science Foundation. Purchase of the X-ray diffractometers was funded by the National Science Foundation (CHE-9105497) and the University of Wisconsin.

## SUPPLEMENTARY MATERIAL AVAILABLE

Tables of crystal data, positional parameters, bond distances and angles, and anisotropic thermal parameters for **1** (7 pages) and for **3**·C<sub>6</sub>H<sub>6</sub> (7 pages) are available. Ordering information is given on any current masthead page.

## REFERENCES

- [1] (a) A. Sekiguchi, T. Yatabe, C. Kabuto, H. Sakurai, *J. Am. Chem. Soc.*, **115**, 1993, 5853 and references therein; (b) N. Wiberg, C. M. M. Finger, K. Polborn, *Angew. Chem., Int. Ed. Engl.*, **32**, 1993, 1054.
- [2] (a) T. Iwahara, R. West, *Chem. Lett.*, 545, 1991; (b) A. Sekiguchi, S. S. Zigler, K. J. Haller, R. West, *Recl. Trav. Chim. Pays-Bas.*, **107**, 1988, 197.
- [3] Y. Wan, J. G. Verkade, *Inorg. Chem.*, **32**, 1993, 341.
- [4] (a) R. F. Trandell, G. Urry, *J. Inorg. Nucl. Chem.*, **40**, 1978, 1305; (b) E. Hengge, *Top. Curr. Chem.*, **51**, 1974, 1; (c) M. Weidenbruch, Y. Pan, K. Peters, H. G. von Schnering, *Chem. Ber.*, **122**, 1989, 885; (d) M. Weidenbruch, Y. Pan, K. Peters, H. G. von Schnering, *Chem. Ber.*, **122**, 1989, 1483.
- [5] J. L. Shibley, R. West, C. A. Tessier, R. K. Hayashi, *Organometallics*, **12**, 1993, 3480.
- [6] (a) D. A. Armitage: in S. Patai, Z. Rappaport, (eds.): *The Silicon-Heteroatom Bond*, Wiley, Chichester, England, pp. 367–485 (1991); (b) R. J. Perry, *Organometallics*, **8**, 1989, 906; (c) D. Seyferth, J. M. Schwark, R. M. Stewart, *Organometallics*, **8**, 1989, 1980; (d) G. H. Wiseman, D. R. Wheeler, D. Seyferth, *Organometallics*, **5**, 1986, 146.
- [7] (a) G. R. Gillette, R. West, *J. Organomet. Chem.*, **394**, 1990, 45; (b) W. Fink, *Helv. Chim. Acta.*, **79** 1963, 721; (c) R. S. Grev, H. F. Schaefer, *J. Am. Chem. Soc.*, **109**, 1987, 6577; (d) D. Cremer, J. Gauss, E. Cremer, *THEOCHEM*, **169**, 1988, 531.
- [8] J. L. Shibley, R. West, J. Belz, R. K. Hayashi, *Organometallics*, in press.
- [9] Y. Kabe, M. Kuroda, Y. Honda, O. Yamashita, T. Kawase, S. Masamune, *Angew. Chem., Int. Ed. Engl.*, **27**, 1988, 1725.
- [10] V. P. Kornilova, E. F. Stefoglo, *Khim. Tekhnol.*, 1990, 19; *Chem. Abs.*, **113**, 99798.
- [11] D. A. Swick, J. L. Karle, *J. Chem. Phys.*, **23**, 1955, 1499.
- [12] L. Pauling: *The Nature of the Chemical Bond*, 3rd ed., Cornell University Press, Ithaca, NY, 1960.
- [13] P. Kosse, E. Popowki, *Z. Anorg. Allg. Chem.*, **613**, 1992, 137.
- [14] F. Vögtle, E. Weber: in S. Patai (ed): *The Chemistry of Ethers, Crown Ethers, Hydroxyl Groups, and Their Sulphur Analogues: Supplement E*, Wiley, Chichester, England, pp. 59–174 (1980).
- [15] A. R. Bassindale, P. G. Taylor, in S. Patai, Z. Rappaport, (eds.): *The Chemistry of Organic Silicon Compound*, Wiley, Chichester, England, pp. 839–892 (1989).
- [16] HCl elimination has been found to occur under very mild conditions. L. W. Breed, R. L. Elliott, *J. Organomet. Chem.*, **11**, 1968, 447.